AIAA-97-0717-

On the Decomposition of Drag Components from Wake Flow Measurements

Timothy T. Takahashi*
NASA Ames Research Center, Moffett Field, California 94035-1000

Drag decomposition, the quantitative separation of drag into components due to viscous and inviscid effects, is explored. Drag is computed from a control volume analysis incorporating a flow field survey made downstream of the test object. The total drag is the aggregate change in streamwise linear momentum. The Betz and Jones equations, for two-dimensional "section drag," are derived as is the Maskell Equation for "profile" and "induced" drag. Many of these equations compute a momentum deficit in a control volume where continuity is not specifically enforced. Experimental data is used to demonstrate the limitations of these computations.

NOMENCLATURE

A projected cross-sectional area
C_D Drag in coefficient form
D_a Axial drag
D_b Betz's profile drag
D_j Jones' profile drag
D_p Profile drag
D_f Fage's profile drag
D_i Inviscid or Induced drag
D_v Vortex drag
D_x Axial drag
D Total drag
d Diameter of circular cylinder
h Total pressure
p Static pressure
q Dynamic pressure
S_0 Upstream plane surface of the control volume, orthogonal to flow
S_1 Downstream plane surface of the control volume orthogonal to flow
S_r Plane surfaces of the control volume, parallel to the flow.
S_∞ Infinite downstream plane surface of the control volume, orthogonal to flow.
u_r velocity component orthogonal to the control volume
u_0,v_0,w_0 components of velocity at surface S_0
u_t velocity component tangential to the control volume
u_1,v_1,w_1 components of velocity at surface S_1
$u_\infty,v_\infty,w_\infty$ components of velocity at surface S_∞
x downstream survey ordinate
ρ density of fluid medium

* National Research Council Postdoctoral Research Scientist Low Speed Aerodynamics Branch, MS 247-2, NASA/Ames Research Center, Moffett Field, Ca., 94035, Member AIAA.

INTRODUCTION

There is a rich history surrounding the experimental determination of aerodynamic drag. Some thirty years after Froude[1] published on the need to streamline ships, man had flown in both heavier than air and lighter than air machines. An interesting method to determine drag is nearly as old; one may indirectly measure drag from its associated momentum loss through a flow survey downstream of the object[2].

From an engineering perspective, it is useful to understand the breakdown of the total drag into components due to viscous and inertial forces so that the mechanisms which cause each can be separately addressed. These drag components are known as the "profile drag" and the "induced drag." Together they represent the total drag :

$$D = D_p + D_i \qquad (1)$$

A major source of confusion to the reader of historical papers concerns a lack of consistency in the definition of words such as "profile drag," "section drag," and "induced drag," or even a precise definition of "total pressure."

A textbook might define the profile drag to be two-dimensional, "section drag," and the induced drag to be the drag-due-to-lift. These definitions are imprecise in terms of the quantitative decomposition process. The author will show that the total drag in a two-dimensional flow, is not necessarily the "section" drag predicted by common formulae. These inconsistencies have lead and will lead to debate.

Consider the noted aerodynamicist, R.T. Jones, who once stated that : "there is no essential relation between lift and induced drag. Consider a flat plate mounted perpendicularly to the ground in a real flow (see Figure 1). The

plate can develop no lift, but there will be a terrible wake with lots of negative pressure and a pair of trailing vorticies."[3]

Wake integral methods comprise one technique by which drag decomposition may be performed. This method is based upon the conservation of linear momentum. A common simplification presumes that airflow is stable and uniform upstream of the object of interest. Downstream, there is a region of undisturbed flow surrounding the viscous wake. The sum of the streamwise components of the forces acting on the fluid within a control volume, the drag, is equal to the change in static pressure and streamwise momentum along the surfaces of the control volume.

There is a substantial body of literature concerning this subject[2,4-33] Most of the debate concerning the applicability of the control volume analysis occurred during the 1930's[4-17]. There were some authors who concerned themselves exclusively with two-dimensional section drag,[4,5,7-11,13,18] and others with the process of drag decomposition[5,20-23,28,30-32]. This paper investigates the applicability of the two-dimensional paradigm upon the process of drag decomposition for three-dimensional flows.

MOMENTUM EQUATIONS

The control volume analysis derives from the inviscid stress tensor; it must have no viscous dissipation along any bounding surfaces. The flow is presumed incompressible and of uniform density. Under these assumptions, the momentum loss is equal to the difference in static pressure and axial linear momentum across the relevant surfaces of the control volume (see Figure 2a). In other words :

$$D = \iint_{S0} p_0 \, dS_0 + \iint_{S0} \rho u_0^2 \, dS_0 - \iint_{S1} p_1 \, dS_1 - \iint_{S1} \rho u_1^2 \, dS_1 - \iint_{Sr} \rho \, u_t \, u_r \, dS_r \qquad (2)$$

At the same time, continuity MUST be enforced:

$$\iint_{S0} \rho u_0 dS_0 - \iint_{S1} \rho u_1 dS_1 - \iint_{Sr} \rho u_t dS_r = 0 \qquad (3)$$

In experiment, the control volume can not be made to extend to the wind tunnel walls. A real wind tunnel has viscous dissipation in the wall boundary layers; this would violate the basic premise of the control volume analysis. An additional complication of viscous wall losses manifests itself in an axial static pressure gradient.

Bollay[4] argues convincingly that, in the limiting case as the control volume becomes very large, the axial velocity along the control volume side walls approaches the upstream axial velocity; $u_1 \Rightarrow u_0$. Substitution of equation (3) into equation (2) results in :

$$D = \iint_{S1} (p_0 - p_1) \, dS_1 - \iint_{S1} \rho \, u_1 (u_0 - u_1) \, dS_1, \qquad (4)$$

an equation which allows for a net mass flux across the surface, S_r. This control volume is represented by Figure 2b.

It is customary practice to measure the flow conditions upstream of a model at a single point, and assume that the measured values for $u0$ and $p0$ are constant over the entire control volume inlet surface. For neither the symmetrical, non-lifting cylinder wake (Figure 4a) nor the asymmetrical high-lift wing wake (Figure 4b) does the downstream dynamic pressure, $q_1 = (1/2) \, \rho \, u_1^2$, outside the viscous wake closely approximate a computed, uniform, upstream dynamic pressure, $q_0 = (1/2) \, \rho \, u_0^2$, necessary for continuity ($u_0 = \iint_{S1} u_1 dS_1 / S_1$). This implies a "thrust," or momentum gain, associated with the flow outside the viscous wake.

These observations reveal a **PARADOX** (see Figure 3). The control volume analysis requires:

* uniform upstream conditions (p_0, h_0),

* isentropy upheld in regions of inviscid flow (Bernoulli's Equation applies along isentropic streamlines; $h_0 = h_1$ outside the viscous wake),

* and, continuity satisfied.

Experimental measurements (refer to Figure 4) show that all three requirements can not be simultaneously satisfied. In order to maintain isentropy and continuity, upstream conditions must be synthesized. If the measured upstream conditions are used, mass does not conserve.

In the case of the lifting geometry (Figure 4b), the dynamic pressure in the wake is greater above the upper surface of the wing than below the lower surface (also see Figure 3c). As can be seen in Figure 5, the total pressure does return to the expected upstream value outside of the viscous wake. While the control volume analysis is applicable behind the cylinder if the Bollay

assumption of $u_1 \Rightarrow u_0$ (equation 4) is used, the same assumption can not be made for the wing wake; the freestream velocities are unsymmetric.

Over the remainder of this manuscript, several different formulae for drag will be derived and applied to experimental data. They include the Bollay decomposition of inviscid drag and profile drag and the two-dimensional Betz and Jones equations. More recently, the Betz equation has been extended for use in highly three-dimensional flows.[20-23,25-27,29,31-33] The applicability of the two-dimensional equations to three-dimensional wakes will be investigated.

BOLLAY DERIVATION OF INVISCID (INDUCED) DRAG

Bollay begins with Equation 4. We define the "induced drag" to be the drag due to inviscid effects. Therefore, the net drag of a purely inviscid flow is the induced drag. This definition is consistent with the induced drag computed from an inviscid code, but is not the drag due to lift. The potential flow must have only doublets and vorticies; there are no net sources or sinks. For a large S_r, and $u_1 \Rightarrow u_0$, continuity states that:

$$\iint_{S0} \rho(u_0 - u_{1i}) dS_0 = \iint_{Sr} \rho u_{ri}\, dS_r = 0 \qquad (5)$$

Upon substitution into Equation (3), the induced drag is represented by:

$$D_i = \iint_{S0} p_0\, dS_0 + \iint_{S0} \rho\, u_0^{\,2}\, dS_0 - \iint_{S1} p_{1i}\, dS_1 - \iint_{S1} \rho\, u_{1i}^2\, dS_1 \qquad (6)$$

Equation (6) may be transformed making use of Bernoulli's equation in three-dimensions) :

$$h = p + (1/2)\rho (u^2+v^2+w^2) \qquad (7)$$

Assuming that the upstream conditions are uniform, and free of vorticity : $v_0 = w_0 = 0$. This allows further simplification to :

$$D_i = \iint_{S0} (h_0 + (1/2)\rho u_0^2)\, dS_0 - \iint_{S1} (h_{1i} + (1/2)\rho(u_{1i}^2 - v_{1i}^2 - w_{1i}^2))\, dS_1 \qquad (8)$$

Resubstitution into Equation (6) results in :

$$D_i = \iint_{S1} (1/2)\, \rho\, (v_{1i}^2 + w_{1i}^2)\, dS_1 + \iint_{S1} (1/2)\, \rho\, (u_0^2 - u_{1i}^2)\, dS_1 \qquad (9)$$

In a flow where there are localized regions of viscous losses, the dominant effect of viscosity is a slowing of the axial flow. Bollay assumes that the cross-plane kinetic energy in the wake is solely due to inviscid effects: $v_{1i} = v_1$ and $w_{1i} = w_1$. The two integrals of the induced drag equation (9) are addressed separately.

The first term of the induced drag expression represents the induced cross-plane kinetic energy, the so called "vortex drag"

$$D_v = \iint_{S1} (1/2)\, \rho\, (v_1^2 + w_1^2)\, dS_1, \qquad (10)$$

and the second term represents the inviscid axial linear kinetic energy losses :

$$D_a = \iint_{S1} (1/2)\, \rho\, (u_0^2 - u_{1i}^2)\, dS_1 \qquad (11)$$

The determination of the magnitude of u_{1i} in a mixed viscous/inviscid flow is a non-trivial task.

BOLLAY DERIVATION OF VISCOUS (PROFILE) DRAG

If the total drag of a body immersed in a real, viscous fluid is known and its inviscid drag is known, the viscous (profile) drag must comprise the difference (equation (1)). Upon combining equations (4) and (9), the profile drag is :

$$D_p = D - D_i = \iint_{S1} (h_0 - h_1)\, dS_1 - \iint_{S1} (1/2)\, \rho\, (u_{1i}^2 - u_1^2)\, dS_1 \qquad (12)$$

The first term is the integrated loss of total pressure:

$$D_f = \iint_{S1} (h_0 - h_1)\, dS_1 \qquad (13)$$

This metric for drag was postulated by Fage[6]. The second term is represents a change in axial kinetic energy:

$$D_x = \iint_{S1} (1/2)\, \rho\, (u_{1i}^2 - u_1^2)\, dS_1 \qquad (14)$$

Recall the paradox. The values of h_0, h_1, p_1, u_1, v_1 and w_1 are defined by the downstream wake survey. There is the dilemma due to the paradox, does one use measured upstream conditions, or computed mass-conservative values for p_0. Either way, the values of Dv and Dp are well defined; they are independent of p_0. There is a twofold uncertainty concerning the proper value of Da and Dx, due to both the value of p_0 and of u_{1i}.

BETZ EQUATION - PROFILE DRAG

The Betz equation[5] was derived, ostensibly, to compute the profile drag of a wing In reality,

it is a method to compute the total drag of an object in a mass-consdervative two-dimensional flow field, a subtle difference. Betz begins with Equation (2), valid for a control volume with no mass flux across S_r. This equation is then rewritten to express drag in terms of a one-dimensional total pressure ($h=p+(1/2)\rho u^2$) :

$$D_b = \iint_{S0} h_0 \, dS_0 + \iint_{S0} (1/2)\, \rho\, u_0^2 \, dS_0 - \iint_{S1} h_1 \, dS_1 - \iint_{S1} (1/2)\, \rho\, u_1^2 \, dS_1 \qquad (15)$$

(N.B. The one-dimensional total pressure defines the total velocity, rather than u_1. Error is dependent upon the local flow angularity. The author uses this definition in order to define the Betz equation as it is commonly written.)

Betz notes that the integrals of total pressure need not be taken over the entire survey. Instead, they are required only in the region of the viscous wake (where $h_1 < h_0$). A second transformation is made, through the introduction of a fictitious velocity, u^*. The motivation for this is to restrict the velocity integration to the viscous wake. This transformation, while introducing a specific source term, does nothing to further address continuity.

The derivation proceeds to define u^* as identical to the real flow outside the viscous wake ($u^* = u_1$) and kinetically equivalent to a drag producing inviscid flow inside the viscous wake ($u^* > u_1$). To maintain continuity (or lack thereof) a source term is introduced whose total yield is : $E = \iint_{S1} (u^* - u_1)\, dS_1$. This source creates a thrust, $-\rho\, u_0\, E$, which must be accounted for. After some algebra, drag is determined to be :

$$D_b = \iint_{S0} (h_0 - h_1)\, dS_0 - \iint_{S0} (1/2)\rho(u^*-u_1)(2\, u_0 - u^* - u_1)\, dS_0 \qquad (16)$$

where :

$$u^* = \sqrt{[\,(2/\rho)(h_0 - p_1)\,]}$$

By the definition of u^*, the domain of both integrals is restricted to that of the viscous wake.

JONES EQUATION - PROFILE DRAG

The Jones equation[8] is derived from equation (4). Recall the assumption of $u_t \Rightarrow u_0$. It allows for non-zero mass flux across the control volume walls, Sr. Up until this point, the control volume has been drawn between an upstream plane, S_0, and a downstream plane, S_1. As momentum must be conserved at all downstream planes, the control volume of interest can be shifted downstream; the inlet at the survey plane, the outlet is now at the Treffetz plane, infinitely far downstream, S_∞, where $p_0=p_\infty$. As such, the momentum equation reduces to :

$$D_j = \iint_{S1} \rho\, u_1 (u_0 - u_\infty)\, dS_1 \qquad (17)$$

In order to estimate u_∞, Jones assumes that the total kinetic energy in the wake remains constant into the extreme far field. If this is true, the velocities may be written (again using a one-dimensional definition of total pressure) as :

$$u_\infty = \sqrt{[\,(2/\rho)(h_1 - p_0)\,]}$$
$$u_0 = \sqrt{[\,(2/\rho)(h_0 - p_0)\,]}$$
$$u_1 = \sqrt{[\,(2/\rho)(h_1 - p_1)\,]}$$

This substitution leads to the Jones equation, as usually seen:

$$D_j = 2 \iint_{S1} \sqrt{[h_1 - p_1]}\,(\sqrt{[h_0 - p_0]} - \sqrt{[h_1 - p_0]})\, dS_1 \qquad (18)$$

Interestingly, an application of Betz's assumptions to equation (4) rather than to equation (2) leads to a complicated expression which lacks the desirable trait of being zero outside of the viscous wake.

EXPERIMENTAL COMPARISION OF METHODS

A calibration data set was obtained for wake profiles behind a circular cylinder of diameter, d=3/4", and aspect ratio 10.6. A seven hole probe was mounted on a traversing mechanism and used to measure the static pressure, true total pressure and flow angularity in the wake[34]. The test was performed at a nominal dynamic pressure of q=8psf, Re=40,000. Schiller[35] determines a drag coefficient of $C_D=D/(Q\,A)$=1.2 at this Reynolds number.

Wake surveys were made over a wide range of downstream survey distances, x, ranging from x/d=0.5 upwards to x/d=37. For x/d>37, the wake had spread sufficiently so that it mingled with the tunnel wall boundary layers. For survey distances of x/d>2.5, the wake appears well formed, with a physically plausible velocity field. Total and static pressure profiles may be seen in Figure 6.

Drag is computed using the following formulae : Betz's equation, Jones' equation and

Fage's simple integration of total pressure. The inlet boundary conditions are computed two ways: 1) non-conservative - $h_0=h_1$ and $p_0=p_1$ outside the viscous wake and 2) conservative - $p_0=h_0-(1/2)\rho u_0^2$ where u_0 enforces continuity and $h0$ enforces isentropy The difference between the methods has a byproduct; the value of q_0 used in the nondimensionalization depends upon the choice of p_0. The results of the drag computations may be seen in Figure 7.

For $x/d>10$, most of the drag equations compute roughly the correct value of drag. The exception is the Betz formula with the continuity enforced upstream boundary conditions. A similar downstream distance dependence was shown by Maull and Bearman[18] for cylinders at Re=35,000. The author refers the reader to Silverstein[14], Davis[17] or Zvannenweld[19] for a comparison of computational methods using a wing wake. When drag is formulated using the measured upstream boundary conditions, the computed coefficients tend towards $C_D=1.2$; for the conservative boundary conditions, $C_D=1.3$. Upon comparison with Schiller[35], one might presume that the non-conservative equations are more accurate in these circumstances.

As can be seen in Figure 7 where $x/d<10$, the formulae become erratic with the non-conservative Jones equation over predicting drag and the others under predicting drag. For $x/d<2.5$, the probe tips are immersed in the recirculation zone of the near wake; the mean downstream velocity measured by the probes is reported as zero. Taylor[11] has shown that the steady state equations were formally applicable only when the survey was made far enough down stream that the static pressure depression in the viscous wake was negligible; this criterion is met for $x/d>10$.

The contribution of the unsteady flow, the Reynolds Stresses, to drag have been neglected in this analysis. High-frequency fluctuations in the flow have an effect upon the computed mean pressures due to the nonlinear transformation of mean probe tip pressures into to engineering parameters (h,p and u). The unsteady flow should conceal additional wake energy. One would anticipate that mean momentum measurements should over predict the momentum deficit in the wake, and hence over predict drag. The only scheme which demonstrates this phenomenon is Jones equation applied with experimental upstream boundary conditions.

EXTENSION INTO THREE DIMENSIONS

The three-dimensional equations for drag may be examined with this knowledge of the results of two-dimensional experiments. Recall that the Betz equation is formally inappropriate for use without mass-conservative upstream conditions. The elegant forms of the two dimensional equations, derived in terms of the one-dimensional total pressure and expressed in terms of the directly measured parameters p and h, are insensitive to flow angularity. These equations should be revised to consider the swirling, vortical flow found in wing wakes.

Many of the recent wake survey experiments at NASA/Ames consider the flow over high-lift systems[36,37]. These tests have investigated the effects of configuration changes upon a high-lift wing. A wing of NACA 63-0215B section vertically spanned the wind tunnel. Semi-span high lift devices, such as Fowler flaps and leading-edge slats were fitted. The wake of this configuration is unusual in that the lift of the basic wing does not express itself as vorticity in the wake; the wake vortex strength is proportional to the change in span loading between the differing wing sections.

The wake of the wing, with main element set to $\alpha=10^o$, and half-span Fowler flap deflected to $d_f=39^o$ relative to the main element is shown in Figures 8a-c. As with the cylinder wake, these measurements were made using a 7-hole probe[34]. The downstream survey was taken orthogonal to the tunnel walls, and located one chord (30") aft of the trailing edge of the flap system.

The differences between the various methods for computing profile drag are assessed using this data. In particular, the two-dimensional Betz equation and the two-dimensional Jones equation may be integrated over the entire experimental grid. As is shown in Table 1, there is strong agreement between Fage and Betz (within 2%). It would appear that the effective magnitude of the Betz "correction" term is small (as Fage noted)[6]. In other words, $u_{1i}\Rightarrow u_1$ and $Dx=0$.

The effects of residual cross-flow are important to the computation of the vortex drag. The vortex drag integrand, $(1/2)\ \rho(v^2+w^2)$, is positive definite; any uniform side flow or downwash will influence this computation. As can be seen in Figure 8c, the vortex drag field computed from the raw wake survey contains a

significant influence from the downwash. The magnitude of these forces may be seen in Table 1. A true representation of the vortical energy may be computed if the mean cross flow velocities are removed from the vortex drag flow field (see Figure 9).

The axial term, D_a, is the most difficult to assess. As can be seen in Figure 8b, the axial velocity defect is very noticeable on the downwash side of the wake and throughout the viscous wake. As noted previously, Da is sensitive to the issue of continuity, the uniformity of the upstream flow, and the Bollay assumption for $u_1 \Rightarrow u_0$. As the integrated difference between numbers of similar magnitude, small changes in the inlet boundary conditions result in large changes in the magnitude of the integrand. For this data set, the result is an apparent thrust and is of similar magnitude to Db, Dj and Dv. As noted previously, the high-lift system has distorted the flow in the tunnel to the extent that the Bollay assumption is no longer valid. To obtain a precise definition of Da, a flow field survey must be taken upstream of the model.

MASKELL'S METHOD

Many recent papers compute drag using the method of Maskell. Maskell performs the decomposition by formulating total drag in three dimensional space, defining Betz's two-dimensional formulation as the profile drag and the remainder as induced drag. Maskell also transforms the induced drag into the stream function/vorticity domain. The axial momentum term, u_{1i}, found in equation (11) and (12), is defined as the Betz momentum correction term.

$$\iint_{S1} (1/2)\, \rho\, (u_{1i}^2 - u_1^2)\, dS_1 = \iint_{S0} (1/2)\, \rho\, (u^* - u)(2\, u_0 - u^* - u_1)\, dS_0$$

Maskell continues the transformation process, expressing the induced drag in terms of a stream function/vorticity decomposition :

$$D_v = \rho/2 \iint_{S_W} \psi\, \xi\, dS_W - \rho/2 \iint_{S_W} \Phi\sigma\, dS_W \qquad (19)$$

where the first term scales with the strength of the vortical flow, and the second term (sometimes omitted)[29] scales with the strength of the residual closure flow in the wake. The necessary terms are computed from the experimental data by defining:

$$\xi = \partial w/\partial y - \partial v/\partial z$$

$$\sigma = \partial v/\partial y + \partial v/\partial z$$

The stream function, ψ, and potential, Φ, are computed as the solutions for the following differential equations :

$$\partial^2\psi/\partial y^2 + \partial^2\psi/\partial z^2 = -\xi \qquad (20)$$

and

$$\partial^2\Phi/\partial y^2 + \partial^2\Phi/\partial z^2 = -\sigma \qquad (21)$$

with impenetrable boundary conditions enforced at the "tunnel walls." The indirect computation of stream function and potential have enforced a zero-dilatation and zero-mean-cross-flow velocity field. In this sense, the transformation is no longer an exact representation of the physical variables. Otherwise, this method is formally equivalent to the primitive variable approach.

The advantage of the Maskell method involves the invariance of the stream function and sigma to uniform cross flow. The disadvantages include a need to differentiate experimental data, and significant computational overhead to solve the Poisson equation. The axial velocity term, previously shown to be troublesome, tends to be discounted as a residual blockage term[22,25,27] or neglected in its entirety[24,26,31].

CONCLUSIONS

The experimental, analytical and computational aspects of drag decomposition have been reviewed. Certain fundamental inconsistencies regarding the derivation of wake integral formulations, specifically those involving the conservation of mass have been revealed. There is a paradox which results from the experimental inability to enforce uniformity, isentropy and continuity between the inlet and outlet of the control volume.

In two dimensions :

* The Betz equation is useful, but easy to misapply (continuity boundary conditions)

* The Jones equation is useful, but easy to misapply ($u_1 \Rightarrow u_0$ boundary conditions).

* When the survey plane is far downstream integrated total pressure loss (Fage), Betz and Jones equations produce similar results.

In three-dimensions :

* Fage (Profile) Drag and Vortex Drag are simple to compute.

* Axial flow Drag is impossible to determine without an upstream flow survey.

The author believes that a strictly primitive variable approach towards the computation of profile drag and vortex drag has benefits of simplicity, especially regarding error analysis. This method has been used recently by Onorato[24] and Chometon and Laurent[28] and Ardonceau and Amani[30].

In terms of usefulness of wake integral drag computations : some authors have found excellent quantitative correlation between wake integral techniques and direct force measurements[29,31,32] while others have shown excellent qualitative, but weaker quantitative correlations.[25,27,30] The author casts his hat in among the second camp. A precise determination of drag is stymied by the need to enforce continuity and/or $u_l \Rightarrow u_0$ boundary conditions, the need to skirt around the PARADOX and the need to account for oft neglected axial momentum terms.

ACKNOWLEDGEMENTS

This research was performed while Dr. Takahashi held a National Research Council/NASA Ames Research Center Associateship.

BIBLIOGRAPHY

[1] Froude, Wm., " The Fundamental Principles Which Govern the Behaviour of Fluids, with Special Reference to the Resistance of Ships," *British Association for the Advancement of Science*, August, 1875.

[2] Taylor, G.I., "Skin Friction on a Flat Surface," British ARC R&M 604, 1918.

[3] Sovran, G., Morel, T. and Mason, W.T., Jr., ed. *Aerodynamic Drag Mechanisms of Bluff Bodies and Road Vehicles*, Plenum, New York, 1978.

[4] Bollay, W. "Determination of Profile Drag from Measurements in the Wake of a Body," *J. Aeronautical Sciences*, Vol. 5, No. 6, p. 247, 1938.

[5] Betz, A. "A Method for the Direct Determination of Wing Section Drag," NACA TM 337 (transl. from *Zeit. fur Flugtechnik*, Feb. 14,1925), 1925.

[6] Fage, A. and Jones, L.J. "On the Drag of an Aerofoil for Two-Dimensional Flow" British ARC, R&M No. 1015, 1925.

[7] Schrenk, M. "Uber Profilwiderstandsmessung im Fluge nach dem Implusverfahren," *Luftfahrt-forschung*, May,1928, p. 1-32, 1928.

[8] Jones, B.M. "Measurement of Profile Drag by the Pitot-Traverse Method," British ARC R&M 1688, 1936.

[9] Doetsch, H. Von, "Profilwiderstandsmessungen in grossen Windkanal der DVL," *Luftfahrt-forschung*, April/May 1937, pp. 173-178,1937.

[10] Muttray, H. "Zuschrift zu dem Bericht von H. Doetsch, Profilewiderstandmessungen im grossen Windkanal der DVL," *Luftfarhrtforschung*, April/May 1937, pp. 371-372, 1937.

[11] Taylor, G.I. "The Determination of Drag by the Pitot Traverse Method," British ARC R&M 1808, 1937.

[12] Squire, H.B. and Young, A.D., "The Calculation of the Profile Drag of Aerofoils," British ARC R&M 1838, 1937.

[13] Fage, A. "Profile and Skin-Friction Aerofoil Drags," British ARC R&M 1852, 1938.

[14] Silverstein, A. "Wake Characteristics and Determination of Profile Drag by the Momentum Method," *Proceedings of the 5th International Conference for Applied Mechanics*, 1938.

[15] Silverstein, A. and Katzoff, S. "A Simplified Method for Determining Wing Profile Drag in Flight," *J. Aeronautical Sciences*, Vol. 7, No. 7, pp. 295-301, 1940.

[16] Rumph, Jr. L.B. and Schairer, R. "Boundary Layer and Wake Survey Measurements in Flight and in the Wind Tunnel," *J. Aeronautical Sciences*, August 1940, pp. 425-433.

[17] Davis, W.F. "Comparision of Various Methods for Computing Drag from Wake Surveys," NACA Wartime Report W-4, 1943.

[18] Maull, D.J. and Bearman, P.W. "The Measurement of the Drag of Bluff Boides by the Wake Traverse Method," *Journal of the Royal Aeronautical Society*, Vol. 68, pg. 843, December 1964.

[19] Zwaaneveld, J. "Comparision of Various Methods for Calculating Profile Drag from Pressure Measurments in the Near Wake at Subcritical Speeds" AGARD Aerospace Drag 10-1, 1973.

[20] Goldstein, S. *Modern Developments in Fluid Mechanics*, Clarendon Press, Oxford, 1938

21 Maskell, E.C. "Progress Towards a Method for the Measuremenbt of the Components of Drag of a Wing of Finite Span," RAE Tech Rep. 72-232, Jan 1973.
22 Wu, J.C., Hackett, J.E. and Lilley, D.E. "A Generalized Wake-Integral Approach for Drag Determination in Three-Dimensional Flows," AIAA Paper 79-0279, 1979.
23 Weston, R.P. , "Refinement of a Method for Determining the Induced and Profile Drag of a Finite Wing from Detailed Wake Measurements" PhD Dissertation, University of Florida, 1981
24 Onorato, M., Costelli, A.F. and Garrone, A. "Drag Measurement through Wake Analysis" SAE Paper 84-0302, 1984.
25 Hackett, J.E. and Sugavanam. A., "Evaluation of a Complete Wake Integral for the Drag of a Car-Like Shape," SAE Paper 84-0577, 1984.
26 Bearman, P.W., "Some Observation on Road Vehicle Wakes," SAE Paper 84-0301, 1984.
27 Hackett, J.E., Williams, J.E. and Patrick, Jr, J. "Wake Traverses Behind Production Cars and Their Interpretation," SAE Paper 85-0280, 1985.
28 Chometon, F. and Laurent, J. ,"Study of Three Dimensional Separated Flows, Relation Between Induced Drag and Vortex Drag," *European Journal of Mechanics B/Fluids*, Vol. 9, No. 5, pp. 437-455, 1990.
29 Brune, G.W. and Bogataj, P.W., "Induced Drag of a Simple Wing from Wake Measurements," SAE Paper 90-1934, 1990.
30 Ardonceau, P. and Amani, G., "Remarks on the Relation Between Lift Induced Drag and Vortex Drag," *European Journal of Mechanics B/Fluids*, Vol. 11, No. 4, pp. 455-460,1992.
31 Brune, G.W., "Quantiative Low-Speed Wake Surveys," *AIAA J. Aircraft*, Vol. 31, No. 2, pp. 249-255,1994.
32 Shoemaker, W., "A Wake Integral Method for Experimental Drag Measurement and Decomposition," PhD Thesis, Stanford University, 1994.
33 McAlister, K.W., Schuler, C.A., Branum, L. and Wu, J.C. "3-D Wake Measurements Near a Hovering Rotor for Determining Profile and Induced Drag," NASA Tech Paper 3577/ATCOM Technical Report 95-A-006, 1995.
34 Takahashi, T.T. , "Measurement of Air Flow Characteristics Using Seven Hole Cone Probes," AIAA Paper 97-0600,1997.
35 Schiller, L. and Linke, W., "Pressure and Frictional Resistance of a Cylinder at Reynolds Numbers 5,000 to 40,000," NACA Tech. Memorandum No. 715, 1933
36 Takahashi, T.T. and Ross, J.C., "On the Development of an Efficient Wake Survey System," SAE Paper 95-1990,1995.
37 Storms, B.L., Takahashi, T.T. and Ross, J.C., "Aerodynamic Influence of a Finite-Span Flap on a Simple Wing," SAE Paper 95-1977,1995.

Table 1 - Drag Computation from Wake Survey NACA 63-0215B wing with half-span flap (α=10,df=39,Re=3,700,000)

FORMULATION		C_D
Df	Fage (Total Pressure) Drag	0.0394
Db	Betz "Profile" Drag (2D)	0.0385
Dj	Jones "Profile" Drag (2D)	0.0483
Da	Axial (non-conservative)	-0.097
Da	Axial (conservative)	-0.052
Dv	Vortex Drag (uncorrected)	0.2879
	Residual Downwash (Clift) :	0.2189
	Residual Sideflow (C_{side})	0.0021
Dv	Vortex Drag (corrected)	0.0669

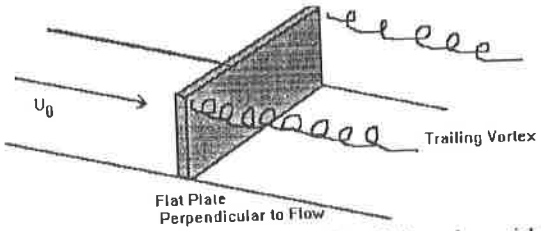

Figure 1 - Flate plate (bluff body) wake with trailing "necklace" vortex. This configuration has finite vortex drag, but zero drag-due-to-lift.

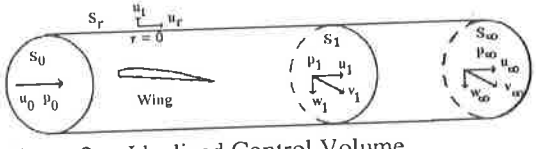

Figure 2a - Idealized Control Volume

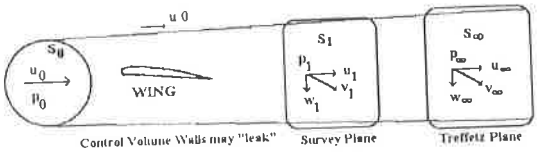

Figure 2b - Bollay's Control Volume

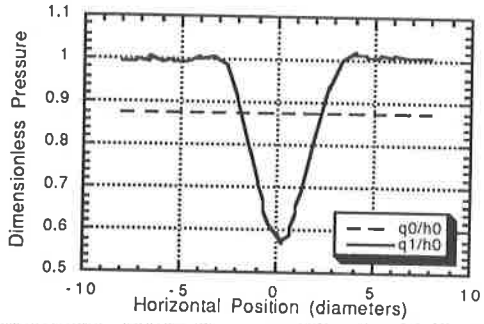

Figure 4a - Wake Survey - Circular Cylinder @ Re=40,000, x/d=9.5. Dynamic pressure, q_1 and synthesized upstream dynamic pressure to enfore continuity, q_0.

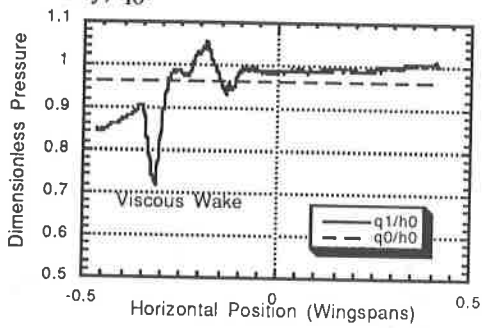

Figure 4b - Wake Survey - Traverse across wake of high-lift wing. α=10°, Re=3,700,000. Dynamic pressure.

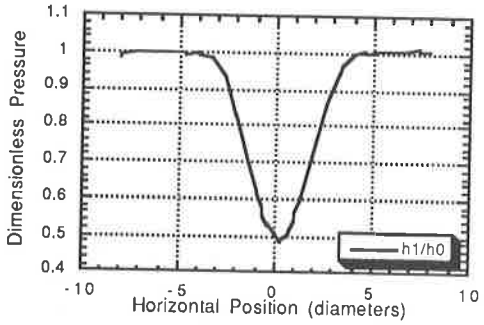

Figure 5a - Wake Survey - Circular Cylinder @ Re=40,000,x/d=9.5. Total pressure defect.

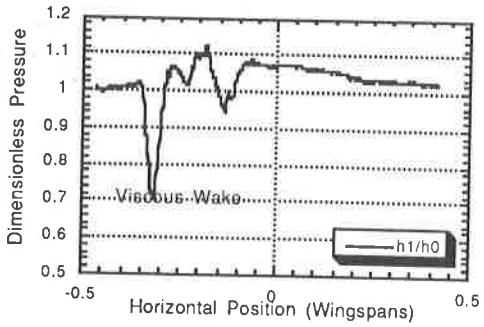

Figure 5b - Wake Survey - High-Lift Wing α=10•, Re=3,700,000. Total pressure defect.

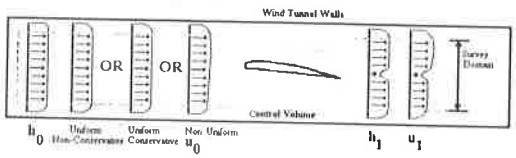

Figure 3 - Control Volume - Paradox Revealed

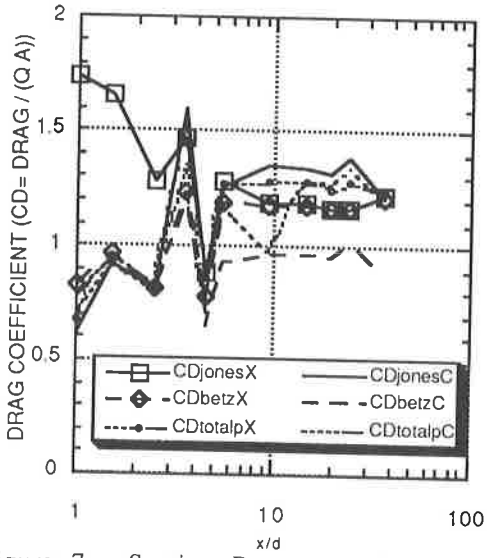

Figure 7 - Section Drag as a function of computational method and downstream survey distance - C - "conservative" upstream boundary conditions, X - "non-conservative" upstream boundary conditions. Cylinder @ Re=40,000.

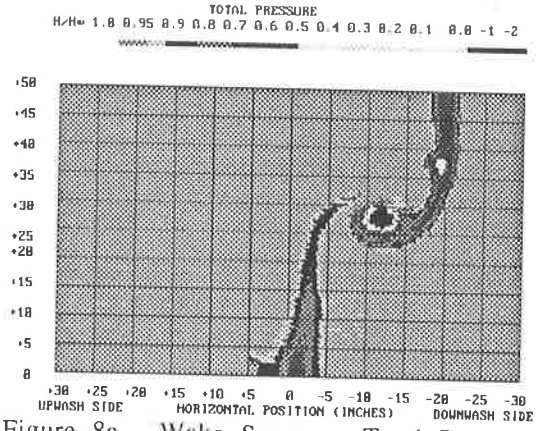

Figure 8a - Wake Survey - Total Pressure Contour - vertically mounted NACA 63-0215B wing with half span flap. Re=3,700,000. Ma=0.22. α= 10°, d_f=39°. h_∞ chosen so h/h_∞=1 outside the viscous wake. Flap mounted on upper half of the wing. Wing and flap "downwash" translates wake to the right.

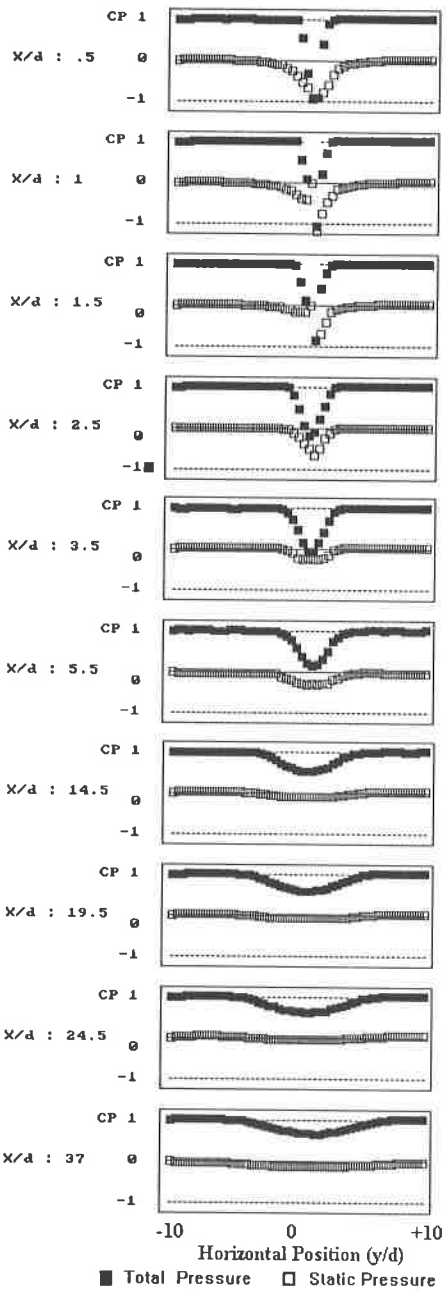

Figure 6 - Static and Total Pressure Profiles Wake of a Circular Cylinder, Re=40,000.

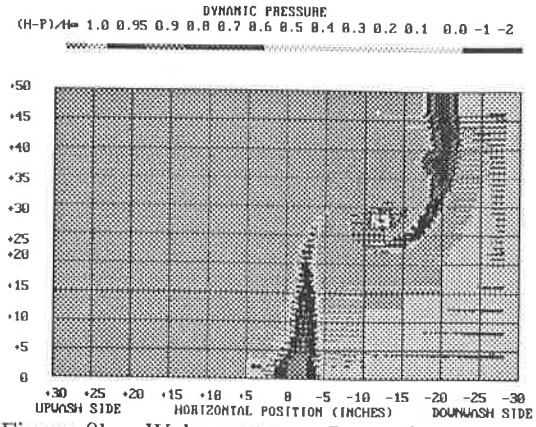

Figure 8b - Wake survey - Dynamic Pressure Contour. h_∞ defined so that $(h-p)/h_\infty=1.0$ on the upwash side of the viscous wake.

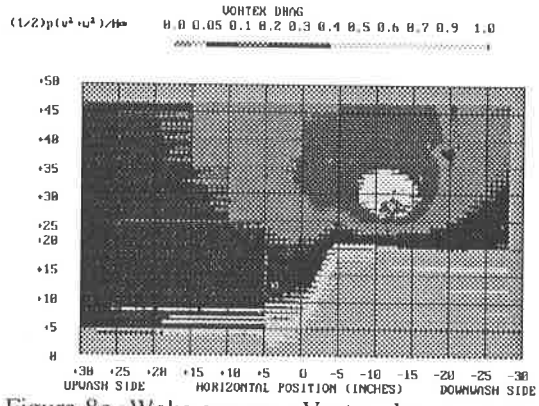

Figure 8c- Wake survey - Vortex drag contours (uncorrected)

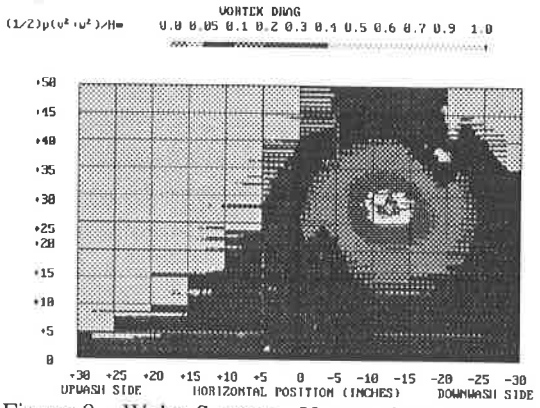

Figure 9 - Wake Survey - Vortex drag contours (corrected to remove uniform cross-flow terms)